


## RESEARCH ARTICLE

# miR-423-3p activates FAK signaling pathway to drive EMT process and tumor growth in lung adenocarcinoma through targeting CYBRD1

Jun Ma<sup>1,2</sup>  | Wuhaio Huang<sup>1</sup> | Chaonan Zhu<sup>3</sup> | Xiaoyan Sun<sup>1</sup> | Qiang Zhang<sup>1</sup> | Lianmin Zhang<sup>1</sup> | Qi Qi<sup>1</sup> | Xiaoming Bai<sup>2</sup> | Yun Feng<sup>2</sup> | Changli Wang<sup>1</sup>

<sup>1</sup>Department of Lung Cancer, Tianjin Medical University Cancer Institute and Hospital, National Clinical Research Center for Cancer, Key Laboratory of Cancer Prevention and Therapy, Tianjin's Clinical Research Center for Cancer, Tianjin, China

<sup>2</sup>Department of Thoracic Surgery, Shanxi Provincial People's Hospital, Taiyuan, China

<sup>3</sup>Department of Thoracic Surgery, North China University of Science and Technology Affiliated Hospital, Tangshan, China

## Correspondence

Jun Ma, Department of Thoracic Surgery, Shanxi Provincial People's Hospital, Taiyuan, Shanxi Province, China.  
Email: pegasus\_2021@126.com

Changli Wang, Department of Lung Cancer, Tianjin Medical University Cancer Institute and Hospital, National Clinical Research Center for Cancer, Key Laboratory of Cancer Prevention and Therapy, Tianjin's Clinical Research Center for Cancer, No.1 Huanhu West Road, North Sports Center, Hexi District, 300202 Tianjin, China.  
Email: wangchangli@tjmuch.com

## Funding information

No funding was received

## Abstract

**Background:** Lung adenocarcinoma (LUAD) is a malignant tumor with a high fatality rate and poor overall survival, while molecular targets diagnosing and alleviating lung cancer remain inadequate.

**Methods:** In this article, we highlighted the upregulation of microRNA-423-3p (miR-423-3p) in LUAD, especially in smokers aged over 40, and revealed that the high expression of miR-423-3p was significantly associated with smoker, age, and pathologic stage of LUAD patients.

**Results:** Moreover, overexpressing miR-423-3p could facilitate LUAD cell proliferation, invasion, adhesion, and epithelial–mesenchymal transition (EMT) process, while depleted miR-423-3p caused repressive influence upon it. Mechanically, we identified that miR-423-3p could activate FAK signaling pathway through binding to the 3'-UTR of cytochrome B reductase 1 (CYBRD1). Furthermore, we demonstrated that CYBRD1 was lowly expressed in LUAD, and miR-423-3p overexpression could rescue the impairment of LUAD cell proliferation, invasion, adhesion, and EMT caused by CYBRD1 depletion. Noticeably, miR-423-3p depletion efficiently hindered LUAD tumor growth *in vivo*.

**Conclusion:** Collectively, our findings demonstrated that miR-423-3p/CYBRD1 axis could be regarded as a promising biomarker to alleviate the poor LUAD prognosis.

## KEYWORDS

cell proliferation, CYBRD1, epithelial–mesenchymal transition, FAK/Paxillin, invasion, lung adenocarcinoma, miR-423-3p

## 1 | INTRODUCTION

Lung cancer is a malignant tumor originated from the bronchial mucosa or glands of the lungs,<sup>1,2</sup> which has characteristics of family clustering and genetic susceptibility.<sup>3,4</sup> According to preventive

pathology, lung cancer is classified into two categories: small cell carcinoma and non-small-cell carcinoma.<sup>5</sup> Among them, non-small-cell carcinoma includes squamous cell carcinoma, adenocarcinoma, and large cell carcinoma.<sup>6</sup> Lung adenocarcinoma (LUAD) is a type of lung cancer, accounting for 40%–55% in all lung cancer cases.

This is an open access article under the terms of the Creative Commons Attribution-NonCommercial License, which permits use, distribution and reproduction in any medium, provided the original work is properly cited and is not used for commercial purposes.

© 2021 The Authors. *Journal of Clinical Laboratory Analysis* published by Wiley Periodicals LLC.

Symptomatically, LUAD is generally accompanied by coughing, wheezing, chest pain, hemoptysis,<sup>7</sup> and brain metastasis.<sup>8</sup> In addition, the occurrence of LUAD is highly related to smoking.<sup>9</sup> Currently, drug therapy, molecular-targeted therapy, and surgical treatment are extensively utilized to alleviate LUAD.<sup>10–12</sup> However, the high recurrence rate of LUAD is primarily responsible for the poor prognosis. Therefore, biomarkers with diagnostic and therapeutic significance are urgently required to predict and alleviate LUAD.

MicroRNA-423-3p (miR-423-3p) belongs to microRNAs, which are defined as small noncoding RNA molecules with single strand.<sup>13</sup> Increasingly, studies have uncovered the functional role of microRNAs in various diseases, such as ischemia-reperfusion injury,<sup>14</sup> human osteoarthritis,<sup>15</sup> and psoriasis.<sup>16</sup> In addition, the research reports about microRNAs have mainly focused on its regulation of multiple cancers, including osteosarcoma,<sup>17</sup> melanoma,<sup>18</sup> and colorectal cancer.<sup>19</sup> As a member of microRNAs, miR-423-3p has been identified as a carcinogenic driver in various cancers. For example, Liu Z et al. revealed the promoted effect of miR-423-3p on cell proliferation and invasion in hepatic cancer,<sup>20</sup> and Guo T et al. verified miR-423-3p as a promising biomarkers in the occurrence and progression of castration-resistant prostate cancer.<sup>21</sup> Recently, miR-423-3p has been proved to participate in lung cancer progression,<sup>22</sup> while the regulatory mechanisms through which tmiR-423-3p involved in LUAD remain uncovered.

Cytochrome B reductase 1 (CYBRD1) belongs to cytochrome b (561) family<sup>23</sup> and is characterized with ferric reductase activity.<sup>24</sup> Based on extensive references, CYBRD1 mainly contributed to the transportation of glucose and other sugars,<sup>25</sup> metal ions, bile salts, and organic acids, as well as the absorption of mineral.<sup>26</sup> CYBRD1 has been proved to be involved in the development of HFE hemochromatosis,<sup>27</sup> chronic hepatitis C,<sup>28</sup> and alcoholic liver disease.<sup>29</sup> Additionally, Lemler DJ et al. demonstrated that DCYTB was a potential biomarker for breast cancer and exerted its functional effect through an iron-independent manner.<sup>30</sup> However, the contribution of CYBRD1 to affecting LUAD has not been revealed.

Thus, we verified the expression levels of miR-423-3p and CYBRD1 and uncovered their regulatory mechanism. Moreover, we investigated the functional influence of miR-423-3p/CYBRD1 axis upon LUAD progression, providing a novel therapeutic candidate for the treatment of LUAD.

## 2 | MATERIALS AND METHODS

### 2.1 | Cell culture and treatment

Human lung adenocarcinoma cell lines NCI-H1299 and NCI-H157, as well as human bronchial epithelial cell line 16HBE, were obtained from ATCC (American Type Culture Collection) and were cultured in indicated medium in accordance with ATCC's instruction. For transfection, the miR-423-3p mimics, miR-423-3p inhibitor, miR-423-3p antagomir, pcDNA-CYBRD1, si-CYBRD1-1, and si-CYBRD1-2 were designed by GeneChem Corporation (Table S1).

### 2.2 | Cell counting kit-8 (CCK-8) and adhesion assay

Cell counting kit-8 was employed in the proliferation assay, NCI-H1299 and NCI-H157 cells were plated into 96-well incubation plates and maintained for 0, 24, 48, or 72 h, and then, the incubation plates were added with CCK-8 solution before 2 h of incubation. A microplate reader was implemented for the measurement of absorption of OD value at 450 nm.

For the estimation of cell adhesive capacity, type I collagen (BD Biosciences) was coated in 6-well plates, and then, the treated plates were utilized to culture NCI-H1299 and NCI-H157 cells for 1h. Then, MTT (Sigma-Aldrich) was supplemented after removing non-adherent cells. At 570 nm, the OD value was measured.

### 2.3 | Transwell

Transwell chambers were utilized for the estimation of NCI-H1299 and NCI-H157 cell invasive capacity. Briefly, the upper chamber was performed for the incubation of these two cell lines, while the lower chamber was supplemented with 10% FBS. Then, cells locating in the upper chamber were performed scrap, and meanwhile, the stain was achieved in the invaded cells derived from the lower chamber utilizing 0.1% crystal violet. An optical microscope (Olympus) was employed to finish the visualization.

### 2.4 | Wound healing

To estimate the migratory capacity, NCI-H1299 and NCI-H157 transfected with indicated plasmids were maintained in 6-well plates for 1 day, followed by finishing the wounds utilizing a pipette tip. After another incubation for 1 day, a microscope (Olympus) was implemented to achieve the collection of images.

### 2.5 | Luciferase reporter assay

For the estimation of the luciferase activity, the wild-type CYBRD1 (CYBRD1-WT) and mutant-type CYBRD1 (CYBRD1-MUT) were, respectively, cloned into a pGL3 luciferase reporter vector (Promega Corporation) containing the Renilla luciferase gene. miR-423-3p mimics or NC mimics were co-transfected with CYBRD1-MUT or CYBRD1-WT luciferase reporter plasmid into NCI-H1299 cells, and the luciferase activity of CYBRD1 was measured utilizing Dual-Luciferase Reporter Assay (Promega).

### 2.6 | RNA immunoprecipitation (RIP)

To determine the relationship between miR-423-3p and CYBRD1, Magna RIP™ RNA Binding Protein Immunoprecipitation Kit

(Millipore) was introduced in RIP assay. In brief, RIP buffer was utilized for the lysis of NCI-H1299 cells, and the cell extract was partly used as an input and partly incubated with anti-Ago2 or anti-IgG-coated beads (Catalog No. 03-110; Millipore) 4°C for 6 h. After the cultivation of specimens with proteinase K buffer, immunoprecipitated RNA was isolated and then was purified. Finally, the CYBRD1 enrichment was measured by qRT-PCR.

## 2.7 | qRT-PCR

To determine the expression levels of miR-423-3p and CYBRD1 in LUAD, the total RNA was isolated adopting TRIzol reagent (Invitrogen), and reverse transcriptase kit (Invitrogen) was introduced for the cDNA synthesis of extracted samples. SYBR Green qPCR Super Mix-UDG (Invitrogen) was employed for qRT-PCR analysis. GAPDH and U6 were considered as internal control. The corresponding primer sequences are elaborated in Table S2.

## 2.8 | Western blotting (WB)

To detect the proteins levels, isolation of extracted proteins was performed utilizing SDS-PAGE, and then, the separated samples were transferred to PVDF membranes incubated in 5% skim milk. Next, these membranes were mixed with primary antibodies at 4°C overnight, mainly containing E-cadherin (ab76055, 1:200), N-cadherin (ab76011, 1:5000), vimentin (ab92547, 1:2000), CYBRD1 (ab66048, 1 ug/mL), p-FAK (ab81298, 1:1000), t-FAK (ab40794, 1:2000), p-Paxillin (ab109547, 1:5000), and t-Paxillin (ab32084, 1:3000) obtained from Abcam (UK) and then were cultured with corresponding secondary antibody conjugated by horseradish peroxidase. Finally, the measurement was conducted employing chemiluminescence system (Bio-Rad).

## 2.9 | RNA pull-down

To verify the correlation between miR-423-3p and CYBRD1, NCI-H1299 cell lysate was mixed with biotin-labeled miR-423-3p, Dynabeads™ M-280 Streptavidin (Invitrogen; Thermo Fisher Scientific) and streptavidin-coated magnetic beads (88817, Invitrogen) at 4°C overnight in RNA pull-down experiments. Then TRIzol® reagent was performed to finish the extraction of RNA fragments bound with beads. The CYBRD1 expression levels were quantified adopting qPCR.

## 2.10 | Xenograft model and IHC staining

To investigate the influence of miR-423-3p on LUAD tumor growth, BALB/c nude mice (5 weeks, 17–21 g) derived from Shanxi Provincial People's Hospital were achieved injection with miR-423-3p-depleted

NCI-H157 cells into the subcutaneous, thereby establishing xenografts tumor models. Then, nude mice were sacrificed mercifully to collect the xenograft tumor tissues after 4 weeks of injection, and the weight and volume (volume (mm<sup>3</sup>) = (L×W<sup>2</sup>)/2 (L: length, W: width)) were measured. All applicable international, national, and/or institutional guidelines for the care and use of animals were followed. This study was approved by Shanxi Provincial People's Hospital.

Xenograft tumor tissues collected from mice were utilized to evaluate the expression of PCNA and CYBRD1 adopting IHC staining. In brief, citrate buffer was performed to achieve the antigen retrieval of tumor tissues, and permeabilization was finished using 0.1% Triton X-100, followed by mixing with anti-PCNA (ab29, 1:20000) and anti-CYBRD1 (ab28758, 2.5 ug/mL) at 4°C overnight. Then, hematoxylin counterstain was performed after the culture with secondary antibody. The images were captured adopting Eclipse 80i (Nikon).

## 2.11 | Informatic analysis

GSE135918 and GSE27486 datasets from the GEO database (<https://www.ncbi.nlm.nih.gov/geo/>). The expression of target miRNAs in LUAD tumor tissues and normal tissue, and clinicopathological parameters (smoker, age, pathologic stage) were downloaded from The Cancer Genome Atlas (TCGA-LUAD) datasets (<https://www.cancer.gov/about-nci/organization/ccg/research/structural-genomics/tcga>). The survival and receiver operating characteristic (ROC) curves were evaluated utilizing miRNA expression levels. The mRNA and protein levels of CYBRD1 and overall survival in LUAD were analyzed through GEPIA2 (<http://gepia.cancer-pku.cn/>). UALCAN database (<http://ualcan.path.uab.edu/index.html>) was used to evaluate the tumor grade. Gene Set Enrichment Analysis (GSEA) was utilized to investigate the CYBRD1-related signaling pathway.

## 2.12 | Statistical analysis

In this work, all data were showed as mean ±SD and were calculated utilizing GraphPad Prism and SPSS. For the difference analysis of groups, Student's *t*-test and one-way analysis of variance (ANOVA) were introduced. The overall survival was analyzed utilizing Kaplan-Meier strategy. *p* < 0.05 presents statistical significance.

# 3 | RESULTS

## 3.1 | Association between miR-423-3p expression and clinicopathological parameters in LUAD patients

To screen the upregulated miRNAs in LUAD patients, we first utilized two cancer datasets GSE135918 and GSE27486 and obtained 7 intersected genes, including hsa-miR-513a-5p, hsa-miR-513b,

hsa-miR-423-3p, hsa-miR-519d, hsa-miR-483-5p, hsa-miR-1298, and hsa-miR-512-5p (Figure 1A). Among them, we noticed that miR-423-3p was obviously upregulated in LUAD tissues according to TCGA-LUAD database analyses (Figure 1B). In addition, we found that the expression level of miR-423-3p was higher in smoked LUAD patients aged over 40 than that in aged <40 patients (Figure 1C). Moreover, survival curve exhibited that the high expression of miR-423-3p was closely associated with poor survival in non-smoked, aged over 65, and pathological stage I LUAD patients (Figure 1D). Interestingly, the ROC curves indicated that miR-423-3p had high clinical diagnostic value for LUAD patients with AUC = 0.826. More specifically, the diagnostic efficiency of miR-423-3p reached a significantly high levels in pathological stage I, aged over 65, and non-smoked LUAD patients, respectively, with AUC = 0.825, AUC = 0.820, and AUC = 0.819 (Figure 1E). Collectively, we suggested that miR-423-3p was highly expressed in LUAD and closely correlated with age, smoking, and pathological stage of LUAD patients.

### 3.2 | miR-423-3p drives LUAD cell proliferation, invasion, adhesion, and EMT

Considering the upregulation of miR-423-3p in LUAD based on informatic analysis, we further examined the expression levels of miR-423-3p in LUAD cell lines (NCI-H1299 and NCI-H157) and human bronchial epithelial cell line 16HBE, and confirmed that miR-423-3p expression was higher in LUAD cell lines than in 16HBE cell (Figure 2A). To further uncover the functional influence of miR-423-3p on LUAD progression, we constructed miR-423-3p-upregulated NCI-H1299 cells and miR-423-3p-depleted NCI-H157 cells (Figure 2B). CCK-8 assay exhibited an accelerated proliferation rate after miR-423-3p overexpression, while miR-423-3p depletion caused markedly inhibited effect upon it (Figure 2C). Similarly, the migratory and invasive capacities of LUAD cells were considerably enhanced by miR-423-3p overexpression and depleted miR-423-3p restrained it (Figure 2D,E). Moreover, upregulated miR-423-3p resulted in the upregulation of N-cadherin and vimentin and the

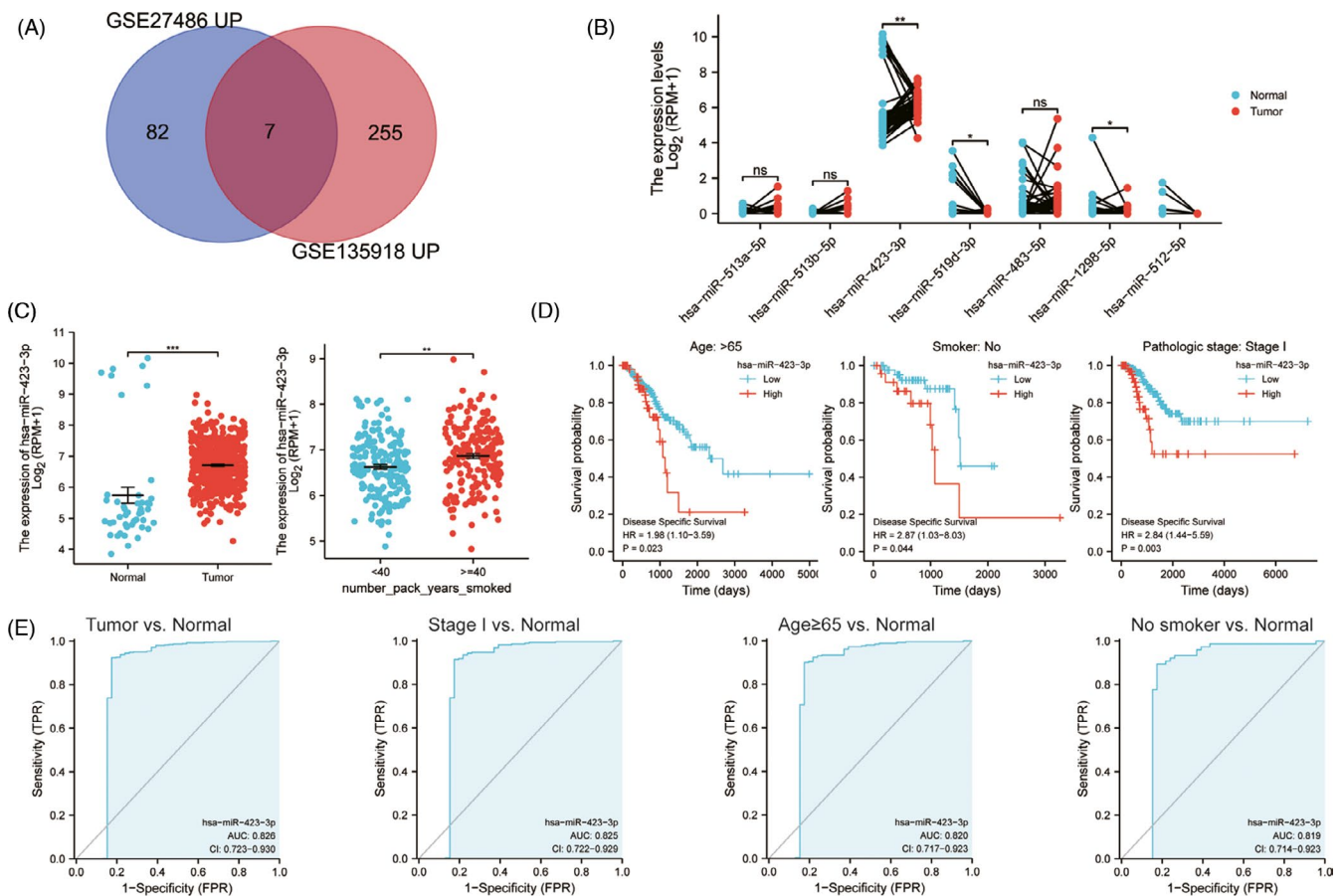


**FIGURE 1** Association between miR-423-3p expression and clinicopathological parameters in LUAD patients. (A) GSE135918 and GSE27486 datasets were adopted for the screen of the upregulated miRNAs in LUAD patients. TCGA database was utilized to analyze the expression of intersected miRNAs (B) and the miR-423-3p-correlated clinicopathological parameters (smoker, age) (C) in LUAD. (D) Survival curves were adopted to analyze the association between miR-423-3p expression and LUAD patients (non-smoking, aged over 65, and pathological stage I). (E) Receiver operator characteristic curve (ROC) curves used to evaluate the diagnostic efficacy of miR-423-3p in LUAD patients

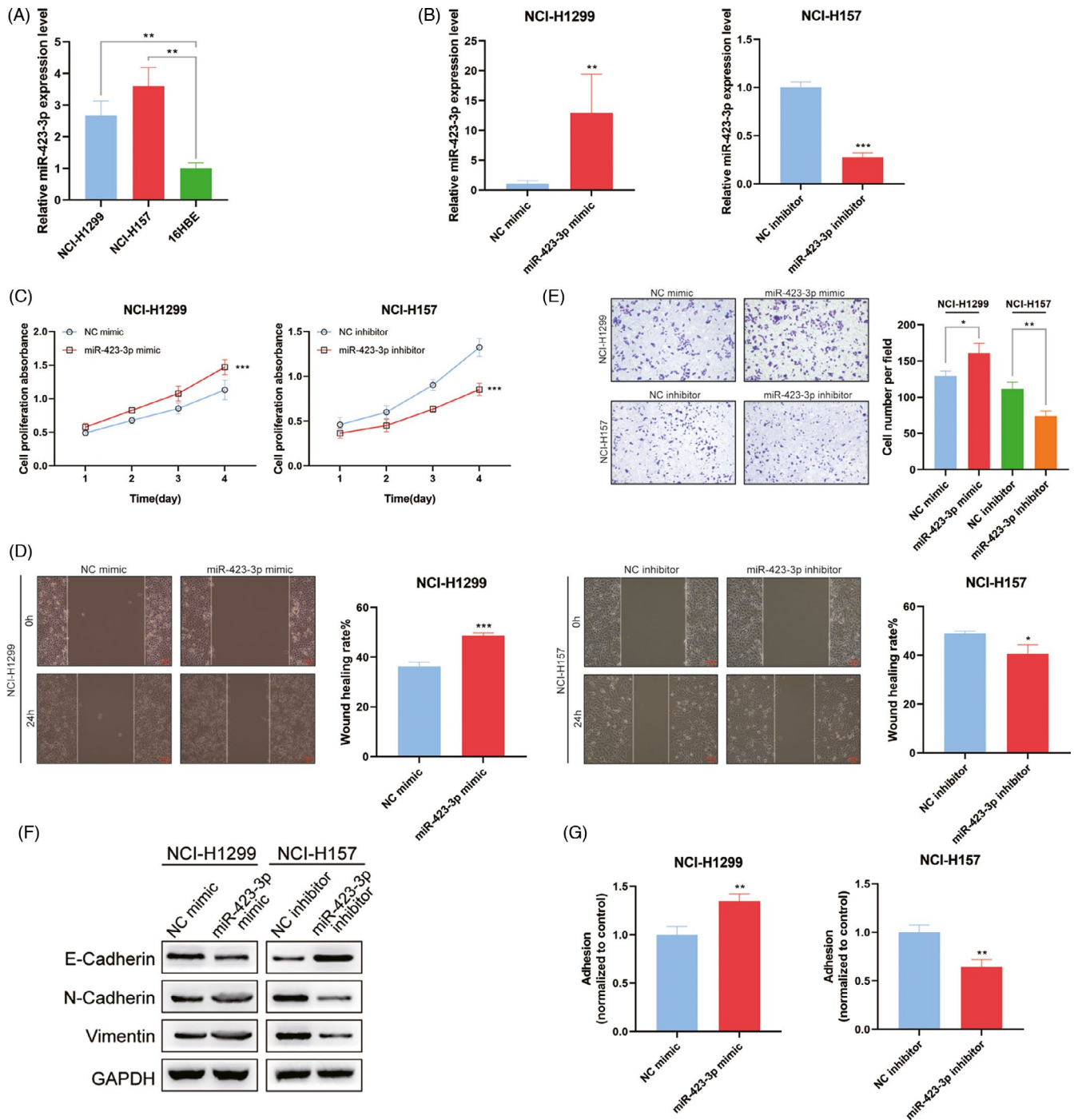


**FIGURE 2** MicroRNA-423-3p facilitates LUAD cell proliferation, invasion, adhesion, and EMT. (A) qRT-PCR was performed for the measurement of miR-423-3p in LUAD cell lines (NCI-H1299 and NCI-H157) and human bronchial epithelial cell line 16HBE. (B) For functional validation, transfection was achieved in NCI-H1299 cells with miR-423-3p mimic plasmid, and in NCI-H157 cells with miR-423-3p inhibitor, qRT-PCR was utilized to examine the transfection efficacy. (C) CCK-8 was performed to detect the proliferation rate of NCI-H1299 and NCI-H157 cells. Wound-healing (D) and Transwell (E) assays were introduced for the cell migration and invasion analyses. Western blotting (F) and adhesion (G) assays were, respectively, employed for the detection of EMT-related proteins and adhesive capacity. \* $p < 0.5$ , \*\* $p < 0.01$ , \*\*\* $p < 0.001$ . Data represent at least three independent sets of experiment

downregulation of E-cadherin, and meanwhile inhibited miR-423-3p exerted reverse impact, concluding that miR-423-3p facilitated the EMT process in LUAD (Figure 2F). In addition, NCI-H1299 cell adhesive ability was promoted by overexpressing miR-423-3p and was obviously hindered by miR-423-3p depletion (Figure 2G). Overall, it was inferred that miR-423-3p played a carcinogenic role in LUAD.

### 3.3 | miR-423-3p targets CYBRD1 in LUAD

To reveal the targeting genes downstream miR-423-3p, we utilized TarBase and GEPIA2 databases to predict the differently downregulated intersection genes and finally screened 42 intersected genes (Figure 3A). We found that CYBRD1 was negatively correlated with



miR-423-3p (Figure 3B). TCGA database further displayed that the mRNA and protein levels of CYBRD1 were markedly upregulated in LUAD tissues (Figure 3C), which could be validated by qPCR assay in LUAD cell lines (Figure 3D).

Subsequently, we found that the mRNA and protein levels of CYBRD1 were significantly attenuated by miR-423-3p overexpression, but were enhanced by miR-423-3p depletion (Figure 3E). Meanwhile, in CYBRD1-WT plasmid transfected NCI-H1299 cells, the luciferase activity of CYBRD1 was efficiently suppressed, while the cells transfected with CYBRD1-MUT had not be impacted (Figure 3F). Furthermore, RIP assay demonstrated that upregulated miR-423-3p could remarkably enrich CYBRD1 in anti-AGO2 complexes (Figure 3G), and the RNA fragments of CYBRD1 could be obviously bound by biotin-labeled miR-423-3p according to RNA pull-down results (Figure 3H). Overall, these data indicated that miR-423-3p could competitively bind to the 3'UTR of CYBRD1 to inhibit its expression in LUAD.

### 3.4 | Confirms the pathological relevance of CYBRD1 in LUAD- and CYBRD1-related signaling pathways

To further investigate the correlation between CYBRD1 expression and clinicopathological parameters in LUAD, we searched TCGA

database and observed that CYBRD1 was significantly downregulated in LUAD smokers aged over 40, and the expression level of CYBRD1 was higher in non-smoked LUAD than smoked ones (Figure 4A). Meantime, with the rise of LUAD tumor stage and grade, the protein levels of CYBRD1 reduced accordingly, indicating that the CYBRD1 expression was negatively correlated with the stage of LUAD tumor (Figure 4A). Additionally, we noticed that the low expression of CYBRD1 indicated poor overall survival and disease-specific survival, and CYBRD1 had a high clinical diagnostic value for LUAD with AUC = 0.886 (Figure 4B), implying that CYBRD1 may act as an indispensable role in LUAD occurrence and progression.

To find out the potential CYBRD1-associated signaling pathway, we first introduced GSEA database and identified 5 primary terms, which were mainly enriched in the negative regulation of epithelial cell apoptotic process, epithelial tube branching in lung morphogenesis, the negative regulation of epithelial cell proliferation, cell cycle, and focal adhesion (Figure 4C). To reveal the CYBRD1-mediated specific signaling pathways, we constructed CYBRD1-upregulated NCI-H157 cells and CYBRD1-silenced NCI-H1299 cells. CYBRD1 silence obviously activated the expression of FAK signaling pathway in NCI-H1299 cells, while CYBRD1 overexpression restrained it (Figure 4D). In summary, CYBRD1 expression was negatively associated with clinicopathological parameters of LUAD and may impact LUAD development through FAK signaling pathway.

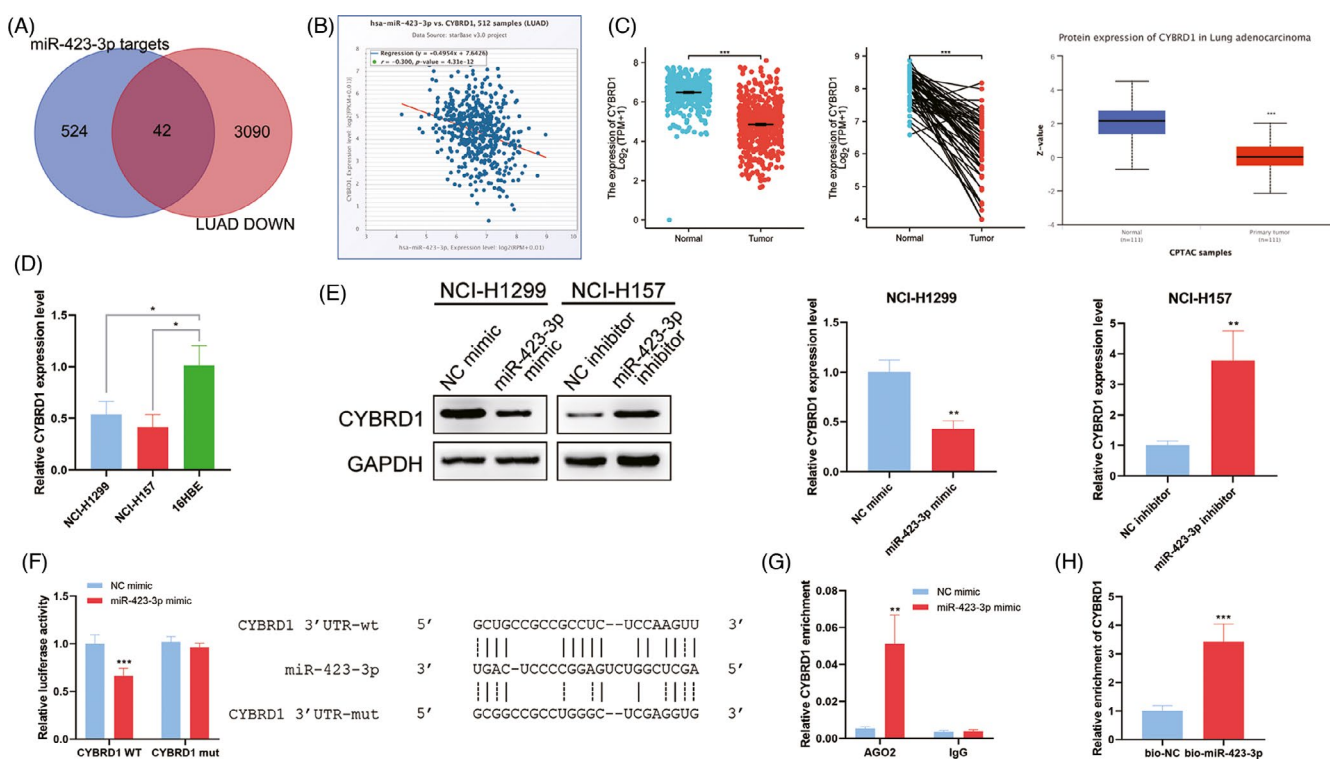


**FIGURE 3** MicroRNA-423-3p inhibits CYBRD1 in LUAD. (A) TarBase and GEPIA2 databases to predict the targeting genes downstream miR-423-3p in LUAD. (B) The correlation analysis between miR-423-3p and CYBRD1 expression. TCGA database (C) and qPCR (D) were adopted to determine the expression of CYBRD1 in LUAD. (E) Western blotting and qPCR were used to measure CYBRD1 expression. (F) Dual-luciferase reporter assay was performed to detect the luciferase activity in NCI-H1299 cells. RIP (G) and RNA pull-down (H) assays were introduced for the validation of correlation between CYBRD1 and miR-423-3p. \* $p < 0.5$ , \*\* $p < 0.01$ , \*\*\* $p < 0.001$ . Data represent at least three independent sets of experiment

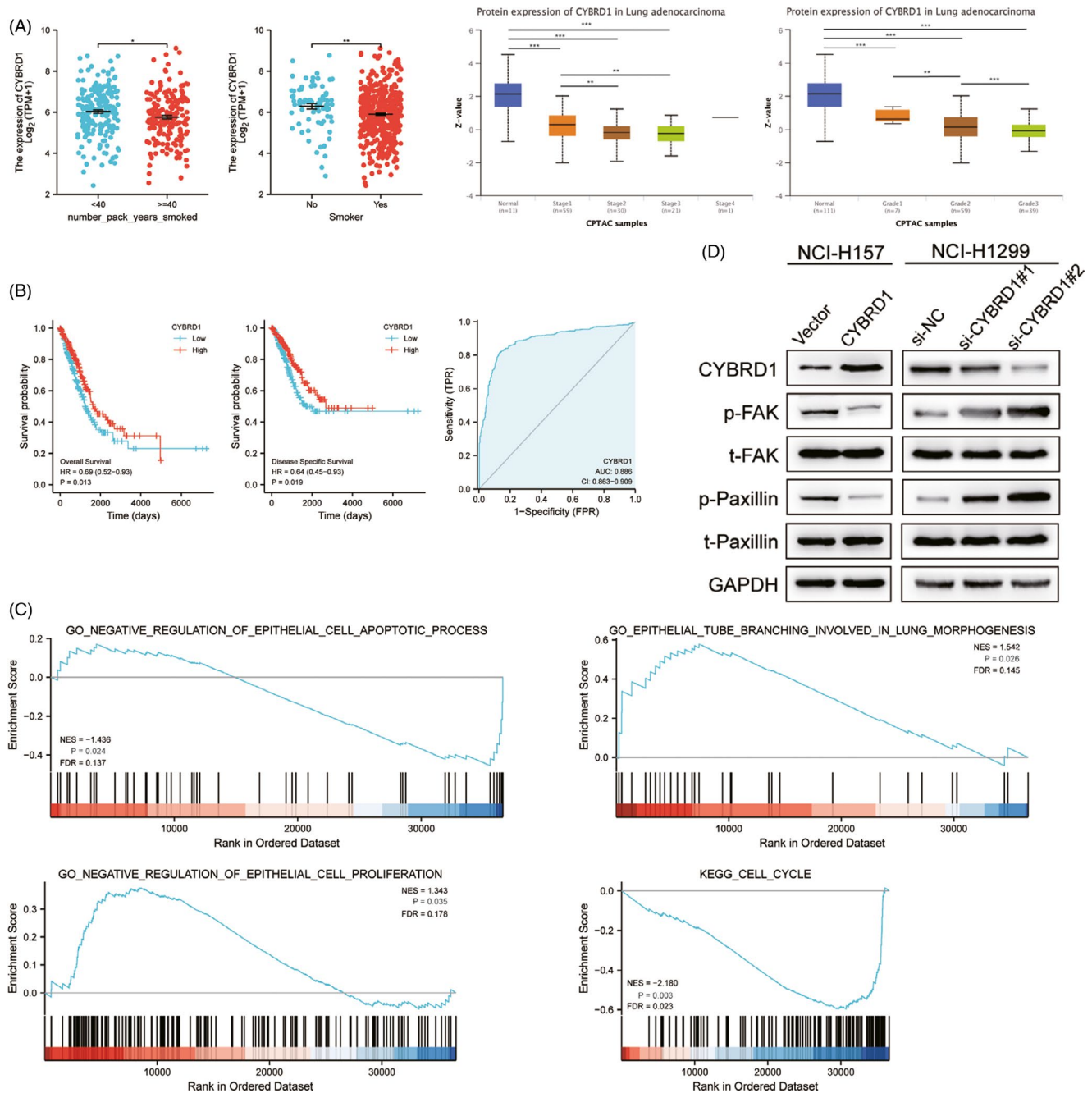


**FIGURE 4** Confirms the pathological relevance of CYBRD1 in LUAD and CYBRD1-related signaling pathways. (A) TCGA database was employed to evaluate the CYBRD1-related clinicopathological parameters (smoker, age, stage, and grade). (B) Overall survival curve was performed to display the correlation between miR-423-3p expression with overall survival and disease-specific survival, and the relationship between CYBRD1 and area under the ROC curve shows that CYBRD1 has the high AUC in LUAD. (C) GSEA database was introduced to predict the CYBRD1-related pathway enrichment. (D) Western blotting was employed to assess FAK signaling pathway. \* $p < 0.5$ , \*\* $p < 0.01$ , \*\*\* $p < 0.001$ . Data represent at least three independent sets of experiment

### 3.5 | miR-423-3p accelerates LUAD cell proliferation, invasion, adhesion, and EMT through targeting CYBRD1

To verify whether miR-423-3p plays a carcinogenic role in LUAD through mediating CYBRD1, we co-transfected miR-423-3p and CYBRD1 overexpression plasmids into NCI-H157 cells. CCK-8

results clarified that CYBRD1 overexpression suppressed NCI-H157 cell proliferation, which could be rescued by upregulated miR-423-3p (Figure 5A). Consistently, wound-healing and Transwell assays also revealed the crucial role of miR-423-3p in recovering the impairment of migration and invasion induced by CYBRD1 (Figure 5B,C). In addition, overexpressing CYBRD1 efficiently hindered the EMT process, FAK/Paxillin pathways, and adhesive viability, while upregulated

miR-423-3p rescued it (Figure 5D,E). Our findings validated that miR-423-3p could facilitate LUAD cell progression and activate the FAK signaling pathway via inhibiting CYBRD1.

### 3.6 | miR-423-3p depletion hinders LUAD tumor growth in vivo

To further confirm whether miR-423-3p impacts LUAD tumor growth in vivo, we established xenograft nude model through injecting miR-423-3p-silenced NCI-H157 cells. We noticed that miR-423-3p silence resulted in a distinctive reduction in LUAD tumor size (Figure 6A,B) and weight (Figure 6C). In addition, depleted miR-423-3p caused the downregulation of miR-423-3p and the upregulation of CYBRD1 in xenograft tumor tissues (Figure 6D). IHC assay displayed that tumor growth-related factor PCNA was evidently restrained in xenograft tumor formed by miR-423-3p-silenced cells, while CYBRD1 was upregulated (Figure 6E). Taken together, we validated that miR-423-3p depletion could exert repressive effect on LUAD tumor growth in vivo.

## 4 | DISCUSSION

Lung adenocarcinoma is a malignant tumor originating from bronchial mucosal epithelium and mucous glands, with poor prognosis

and high recurrence rate.<sup>31</sup> Up to date, enormous biomarkers have been revealed to be capable of impacting the occurrence and progression of LUAD. Among them, microRNAs have been regarded as indispensable mediators in LUAD. For example, Yu F and colleagues demonstrated that exosomal miR-31-5p derived from hypoxic tumor targeted SATB2 and activated MEK/ERK signaling to facilitate tumor metastasis in LUAD,<sup>32</sup> and Zhan J et al. demonstrated that miR-3130-5p could drive the growth, metastasis, and EMT progress in LUAD through directly mediating NDUFS1.<sup>33</sup> In addition, Liu H et al. revealed the carcinogenic role of miR-301b-3p in inducing LUAD cell proliferation, migration, and invasion via inhibiting DLC1.<sup>34</sup> Consistent with previous research, we found that miR-423-3p was highly expressed in LUAD and the high expression miR-423-3p predicted poor survival probability in non-smoked, aged over 65, and pathological stage 1 LUAD patients. More importantly, we also determined miR-423-3p as a carcinogenic driver due to its promoted effect on LUAD cell proliferation, migration, invasion, and adhesion, and in vivo, we demonstrated that miR-423-3p silence could efficiently restrain xenograft tumor growth. EMT has been identified as the transformation of epithelial-to-mesenchymal cells, which impart the capacity of cells to migrate and invade.<sup>35</sup> Herein, we found that miR-423-3p caused the upregulation of EMT-related proteins (N-cadherin and vimentin), thereby accelerating the EMT progress, which further explained the reason why miR-423-3p promotes LUAD cell proliferation and migration.

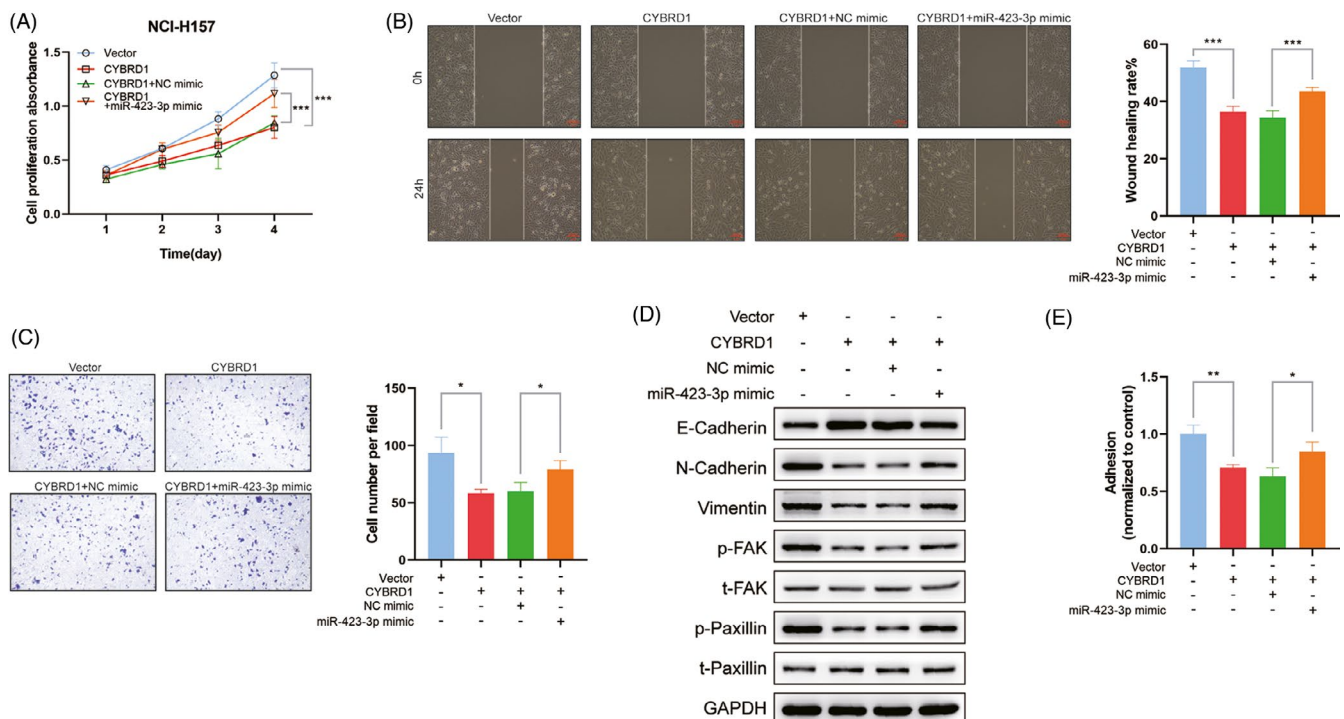


**FIGURE 5** MicroRNA-423-3p facilitates LUAD cell proliferation, invasion, adhesion, and EMT via inhibiting CYBRD1. NCI-H157 cells were co-transfected with miR-423-3p and CYBRD1 overexpression plasmids. (A) CCK-8 was performed to detect the proliferation rate of NCI-H157 cells. Wound-healing (B) and Transwell (C) assays were, respectively, introduced to estimate NCI-H157 cell migration and invasion. Western blotting (D) and adhesion (E) assays were respectively employed to examine EMT-related protein expression and adhesive rate. \* $p < 0.5$ , \*\* $p < 0.01$ , \*\*\* $p < 0.001$ . Data represent at least three independent sets of experiment



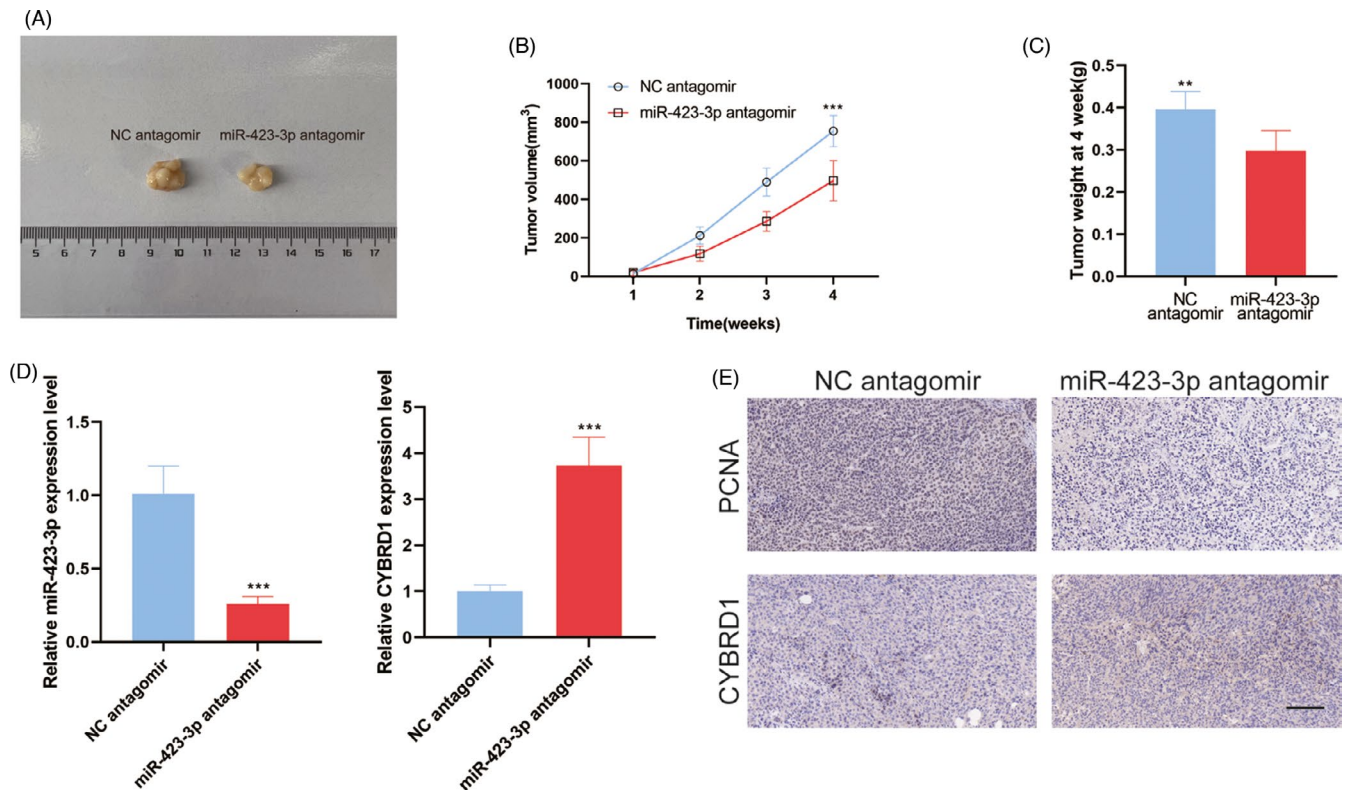


**FIGURE 6** MicroRNA-423-3p depletion restrains LUAD tumor growth in vivo. Xenograft nude model was conducted through injecting miR-423-3p-silenced NCI-H157 cells to assess the tumor size (A and B) and weight (C). (D) qPCR was performed to detect miR-423-3p and CYBRD1 expression in tumor tissues. (E) IHC assay was introduced to measure the levels of PCNA and CYBRD1 in xenograft tumor

According to previous research, CYBRD1 has been proved mainly involved in the regulation of the transportation of metal ions<sup>36</sup>; in addition, Velázquez-Fernández D et al. revealed that CYBRD1 was downregulated in adrenocortical neoplasms.<sup>37</sup> In our work, we found that CYBRD1 was obviously downregulated in LUAD tissues based on TCGA-LUAD database. Combining with bioinformatic analysis and cell experiments, CYBRD1 expression was negatively correlated with miR-423-3p, and miR-423-3p could competitively bind to the 3'-UTR of CYBRD1 to repress its expression. Moreover, the low expression of CYBRD1 predicted poor overall survival and disease-specific survival in LUAD, and CYBRD1 depletion caused the activation of FAK signaling pathway. FAK/Paxillin pathway has been demonstrated to be responsible for cell adhesion,<sup>38</sup> and as a confirmation, we found that silencing CYBRD1 could restrain LUAD cell adhesive capacity. Furthermore, we verified that CYBRD1 overexpression could impair the LUAD cell proliferation, invasion, adhesion, and EMT process, which could be rescued by miR-423-3p overexpression, determining that miR-423-3p could drive LUAD progression via CYBRD1.

To summarize, we highlighted the upregulation of miR-423-3p and the downregulation of CYBRD1 in LUAD and determined CYBRD1 as the target gene of miR-423-3p. Functionally, miR-423-3p facilitated LUAD cell proliferation, invasion, adhesion, and EMT progress via binding to CYBRD1. These findings verified miR-423-3p/CYBRD1 as the promising and actionably biomarkers for diagnosing and alleviating LUAD.

## ACKNOWLEDGEMENTS

None.

## CONFLICT OF INTEREST

The authors declare that they have no competing interests.

## DATA AVAILABILITY STATEMENT

My manuscript has no associated data.

## ORCID

Jun Ma  <https://orcid.org/0000-0002-5242-8848>

## REFERENCES

- Molina J, Aubry M, Lewis J, et al. Primary salivary gland-type lung cancer: spectrum of clinical presentation, histopathologic and prognostic factors. *Cancer*. 2007;110(10):2253-2259.
- Woolner L, Fontana R, Cortese D, et al. Roentgenographically occult lung cancer: pathologic findings and frequency of multicentricity during a 10-year period. *Mayo Clin Proc*. 1984;59(7):453-466.
- McDuffie H. Clustering of cancer in families of patients with primary lung cancer. *J Clin Epidemiol*. 1991;44(1):69-76.
- Bennett W, Alavanja M, Blomeke B, et al. Environmental tobacco smoke, genetic susceptibility, and risk of lung cancer in never-smoking women. *J Natl Cancer Inst*. 1999;91(23):2009-2014.
- Relli V, Trerotola M, Guerra E, Alberti S. Abandoning the notion of non-small cell lung cancer. *Trends Mol Med*. 2019;25(7):585-594.
- Vashi R, Patel B. Roles of ARF tumour suppressor protein in lung cancer: time to hit the nail on the head! *Mol Cell Biochem*. 2021;476(3):1365-1375.

7. Ellis PM, Vandermeer R. Delays in the diagnosis of lung cancer. *J Thorac Dis.* 2011;3(3):183.
8. Fu F, Zhang Y, Gao Z, et al. Development and validation of a five-gene model to predict postoperative brain metastasis in operable lung adenocarcinoma. *Int J Cancer.* 2020;147(2):584-592.
9. Zhang M, Huo C, Jiang Y, et al. AURKA and FAM83A are prognostic biomarkers and correlated with tumor-infiltrating lymphocytes in smoking related lung adenocarcinoma. *J Cancer.* 2021;12(6):1742-1754.
10. Zhang H, Guo L, Chen J. Rationale for Lung Adenocarcinoma Prevention and Drug Development Based on Molecular Biology During Carcinogenesis. *Oncotargets Ther.* 2020;14(13):3085-3091.
11. Haber D, Bell D, Sordella R, et al. Molecular targeted therapy of lung cancer: EGFR mutations and response to EGFR inhibitors. *Cold Spring Harb Symp Quant Biol.* 2005;70(0):419-426.
12. Bains MS. Surgical treatment of lung cancer. *Chest.* 1991;100(3):826-837.
13. Ha M, Kim VN. Regulation of microRNA biogenesis. *Nat Rev Mol Cell Biol.* 2014;15(8):509-524.
14. Luo C, Ling G, Lei B, et al. Circular RNA PVT1 silencing prevents ischemia-reperfusion injury in rat by targeting microRNA-125b and microRNA-200a. *J Mol Cell Cardiol.* 2021;159:80-90.
15. Zhu H, Zhu S, Shang X, et al. Exhausting circ\_0136474 and restoring miR-766-3p attenuate chondrocyte oxidative injury in IL-1 $\beta$ -induced osteoarthritis progression through regulating DNMT3A. *Front Genet.* 2021;12:648709.
16. Zhang W, Yi X, An Y, et al. MicroRNA-17-92 cluster promotes the proliferation and the chemokine production of keratinocytes: implication for the pathogenesis of psoriasis. *Cell Death Dis.* 2018;9(5):567.
17. Han G, Guo Q, Ma N, et al. LncRNA BCRT1 facilitates osteosarcoma progression via regulating miR-1303/FGF7 axis. *Aging.* 2021;13:15501-15510.
18. Xu Y, Guo B, Liu X, Tao K. miR-34a inhibits melanoma growth by targeting ZEB1. *Aging.* 2021;13:15538-15547.
19. Liu Z, Lu T, Wang Y, et al. Establishment and experimental validation of an immune miRNA signature for assessing prognosis and immune landscape of patients with colorectal cancer. *J Cell Mol Med.* 2021;25(14):6874-6886.
20. Liu Z, Cui Y. Bim's effect on the expression of miR-423-3p in promoting primary hepatic cancer (PHC) and role of miR-423-3p in PHC proliferation and invasion. *Biochem Genet.* 2021;59(5):1247-1259.
21. Guo T, Wang Y, Jia J, et al. The identification of plasma exosomal miR-423-3p as a potential predictive biomarker for prostate cancer castration-resistance development by plasma exosomal miRNA sequencing. *Front Cell Dev Biol.* 2020;8:602493.
22. Liu Y, Huang R, Xie D, Lin X, Zheng L. ZNF674-AS1 antagonizes miR-423-3p to induce G0/G1 cell cycle arrest in non-small cell lung cancer cells. *Cell Mol Biol Lett.* 2021;26(1):6.
23. Asard H, Barbaro R, Trost P, Bérczi A. Cytochromes b561: ascorbate-mediated trans-membrane electron transport. *Antioxid Redox Signal.* 2013;19(9):1026-1035.
24. Gunshin H, Starr CN, DiRenzo C, et al. Cybrd1 (duodenal cytochrome b) is not necessary for dietary iron absorption in mice. *Blood.* 2005;106(8):2879-2883.
25. Vlachodimitropoulou E, Sharp PA, Naftalin RJ. Quercetin-iron chelates are transported via glucose transporters. *Free Radic Biol Med.* 2011;50(8):934-944.
26. Liu W, Wen D, Liu Z, Wang K, Wang J. Genetic characteristics of systematic juvenile idiopathic arthritis and the bioinformatics basis for treatment. 2021.
27. Jacolot S, Yang Y, Paitry P, Férec C, Mura C. Iron metabolism in macrophages from HFE hemochromatosis patients. *Mol Genet Metab.* 2010;101:258-267.
28. Rudnicka A, Woziwodzka A, Wróblewska A, et al. Analysis of polymorphism and hepatic expression of duodenal cytochrome b in chronic hepatitis C. *J Gastroenterol Hepatol.* 2017;32(2):482-486.
29. Dostalíková-Cimbuřová M, Balusíková K, Krátka K, et al. Role of duodenal iron transporters and hepcidin in patients with alcoholic liver disease. *J Cell Mol Med.* 2014;18(9):1840-1850.
30. Lemler D, Lynch M, Tesfay L, et al. DCYTB is a predictor of outcome in breast cancer that functions via iron-independent mechanisms. *Breast Cancer Res.* 2017;19(1):25.
31. Auerbach O, Forman J, Gere J, et al. Changes in the bronchial epithelium in relation to smoking and cancer of the lung; a report of progress. *N Engl J Med.* 1957;256(3):97-104.
32. Yu F, Liang M, Huang Y, Wu W, Zheng B, Chen C. Hypoxic tumor-derived exosomal miR-31-5p promotes lung adenocarcinoma metastasis by negatively regulating SATB2-reversed EMT and activating MEK/ERK signaling. *J Exp Clin Cancer Res.* 2021;40(1):179.
33. Zhan J, Sun S, Chen Y, et al. MiR-3130-5p is an intermediate modulator of 2q33 and influences the invasiveness of lung adenocarcinoma by targeting NDUFS1. *Cancer Med.* 2021;10(11):3700-3714.
34. Liu H, Ma X, Niu N, et al. MIR-301b-3p promotes lung adenocarcinoma cell proliferation, migration and invasion by targeting DLC1. *Technol Cancer Res Treat.* 2021;20:1533033821990036.
35. Tian Y, Zhang L, Liu F, et al. Multi-stage responsive peptide nanosensor: anchoring EMT and mitochondria with enhanced fluorescence and boosting tumor apoptosis. *Biosens Bioelectron.* 2021;184:113235.
36. Repo M, Hannula M, Taavela J, et al. Iron transporter protein expressions in children with celiac disease. *Nutrients.* 2021;13(3):776.
37. Velázquez-Fernández D, Laurell C, Geli J, et al. Expression profiling of adrenocortical neoplasms suggests a molecular signature of malignancy. *Surgery.* 2005;138(6):1087-1094.
38. Kafi M, Aktar K, Todo M, Dahiya R. Engineered chitosan for improved 3D tissue growth through Paxillin-FAK-ERK activation. *Regen Biomat.* 2020;7(2):141-151.

## SUPPORTING INFORMATION

Additional supporting information may be found in the online version of the article at the publisher's website.

**How to cite this article:** Ma J, Huang W, Zhu C, et al. miR-423-3p activates FAK signaling pathway to drive EMT process and tumor growth in lung adenocarcinoma through targeting CYBRD1. *J Clin Lab Anal.* 2021;35:e24044. <https://doi.org/10.1002/jcla.24044>